Sideward Stimulated Raman Scattering of a Short Laser Pulse in a Plasma Channel

Stimulated Raman scattering (SRS)[1] is the decay of an incident, or pump, light wave (0) into a frequency-downshifted, or Stokes, light wave (1) and an electron-plasma wave (2). The conservation of energy and momentum in this decay is signified by the frequency and wave-vector matching conditions

$$\omega_0 = \omega_1 + \omega_2, \quad \mathbf{k}_0 = \mathbf{k}_1 + \mathbf{k}_2 , \tag{1}$$

in which $(\omega_0,\mathbf{k}_0)$ and $(\omega_1,\mathbf{k}_1)$ satisfy the dispersion relation $\omega = \left(\omega_e^2 + c^2k^2\right)^{1/2}$, where ω_e is the electron-plasma frequency,[1] and $(\omega_2,\mathbf{k}_2)$ satisfies the dispersion relation $\omega = \omega_e$. The wave-vector matching condition is illustrated in Fig. 71.24(a).

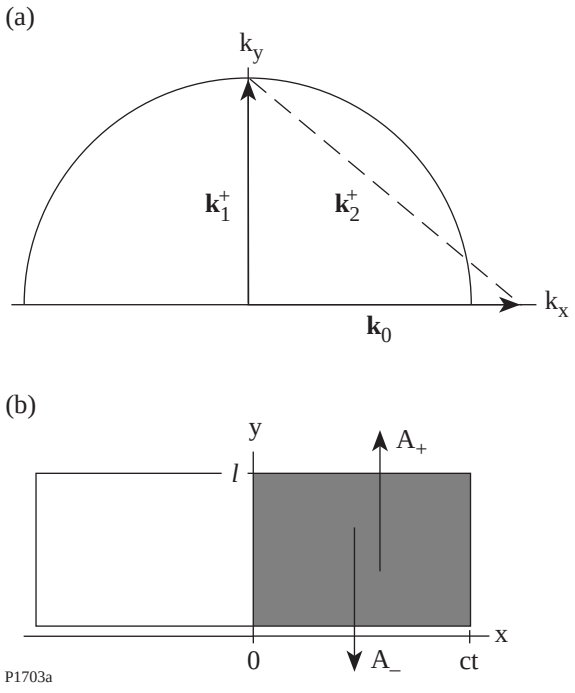

Figure 71.24
Geometry of sideward SRS. (a) Wave-vector diagram for the upward (+) decay. The wave-vector diagram for the downward (–) decay is similar. (b) Region of the plasma illuminated by the laser pulse.

The SRS of a short laser pulse is important in the contexts of particle acceleration[2] and inertial confinement fusion.[3,4] In previous studies of the spatiotemporal evolution of SRS,[5–13] the Stokes waves were allowed to pass freely through the pulse boundaries. However, the radial ponderomotive force associated with the pulse can expel plasma from the neighborhood of the pulse axis, in which case SRS occurs in a plasma channel.[14] A channel can also be preformed by a second pulse.[15] The reflection of light by the channel walls couples Stokes waves propagating symmetrically relative to the pulse axis, as shown in Fig. 71.24(b), and enhances the growth of oblique SRS.

In this study we investigate the effects of reflections on sideward SRS in a plasma channel. Sideward SRS is a useful paradigm of oblique SRS because its two-dimensional geometry is representative of oblique SRS, but simple enough to preclude some of the mathematical complications associated with oblique SRS.[13] To analyze SRS in an optical fiber, one decomposes the radial structure of the waves into the eigenmodes of the fiber.[16] We avoid the difficulties associated with the determination of the (evolving) channel profile and the associated radial eigenmodes by using an empirical parameter r to characterize reflections from the channel walls.[17]

Mathematical Analysis

In the weak-coupling regime, the initial evolution of sideward SRS in an underdense plasma is governed by the linearized equations

$$\left(\partial_t \pm c\partial_y\right)A_\pm = \gamma_0 N_\pm, \quad \partial_t N_\pm = \gamma_0 A_\pm , \tag{2}$$

where $A_\pm$ represents the vector potentials associated with the Stokes waves, $N_\pm$ represents the density fluctuations associated with the electron-plasma waves, and $\gamma_0 = \omega_2 c\left|\mathbf{k}_2\right| A_0/4\left(\omega_0\omega_2\right)^{1/2}$ is the temporal growth rate of SRS in an infinite plasma.[1] It is advantageous to define the characteristic variables $\tau = (ct - x)/l$ and $\eta = y/l$, in terms of which Eqs. (2) become

$$\left(\partial_\tau \pm \partial_\eta\right) A_\pm = \gamma N_\pm, \quad \partial_\tau N_\pm = \gamma A_\pm, \tag{3}$$

where $\gamma = \gamma_0 l/c$.[18] These equations are to be solved subject to the initial conditions

$$A_\pm(0,\eta) = 0, \quad N_\pm(0,\eta) = 1, \tag{4}$$

which are representative of a pulse convecting into fresh plasma, in which a constant level of density fluctuations is available to seed the instability, and the boundary conditions

$$A_+(\tau,0) = r\,A_-(r,0), \quad A_-(\tau,1) = r\,A_+(\tau,1). \tag{5}$$

It follows from Eqs. (3)–(5) that $A_-(\tau,\eta) = A_+(\tau,1-\eta)$ and $N_-(\tau,\eta) = N_+(\tau,1-\eta)$. Consequently, only the solutions for A_+ and N_+ will be stated explicitly.

One can solve Eqs. (3)–(5) by using Laplace transforms. For the special case in which r = 0 the wave amplitudes are given by

$$A_+(\tau,\eta) = \begin{cases} \sinh(\gamma\tau), \\ \sum_{n=0}^{\infty} F_{2n+1}(\tau,\eta), \end{cases} \qquad N_+(\tau,\eta) = \begin{cases} \cosh(\gamma\tau), \\ \sum_{n=0}^{\infty} F_{2n}(\tau,\eta), \end{cases} \tag{6}$$

where

$$F_n(\tau,\eta) = \left[\eta/(\tau-\eta)\right]^{n/2} I_n\left\{2\gamma\left[\eta(\tau-\eta)\right]^{1/2}\right\} \tag{7}$$

and I_n is the modified Bessel function of order n. The first forms of Eqs. (6) are valid for $\tau \le \eta$ and the second forms are valid for $\tau > \eta$. At any point (x,y) in the plasma, the pulse arrives and initiates the instability at $t = x/c$, after which the Stokes amplitude experiences exponential growth with growth rate γ_0. The information that the side boundary at y = 0 is present reaches that point at $t = (x+y)/c$, after which the Stokes wave experiences Bessel growth. Since $I_n(z) \approx \exp(z)/(2\pi z)^{1/2}$ when $z >> 1$, the Stokes amplitude grows in proportion to $\exp\left[2\gamma_0 (yt/c)^{1/2}\right]$ when $t >> (x+y)/c$. At these late times, $t >> (yt/c)^{1/2}$. Thus, *the sideward convection of the Stokes wave converts fast exponential growth to slow Bessel growth*. A snapshot of the Stokes amplitude is displayed in Fig. 71.25(a) for the case in which $ct/l = 2$ and $\gamma_0 l/c = 2$.[19] The transition from one-dimensional exponential growth to two-dimensional Bessel growth is evident.

For the special case in which $r = 1$, the wave amplitudes are given by

$$A_+ = \sinh(\gamma\tau), \quad N_+ = \cosh(\gamma\tau). \tag{8}$$

Thus, *the total reflection of the Stokes light maintains the fast exponential growth of sideward SRS, even after the information that the pulse boundaries are present has reached the pulse interior*. A snapshot of the Stokes amplitude is displayed in Fig. 71.25(b) for the case in which $ct/l = 2$ and $\gamma_0 l/c = 2$. It is evident that total reflection allows the wave evolution to remain one-dimensional and enhances the wave growth. What must be determined is how large a reflectivity is needed to have a significant effect.

For the general case in which 0 < r < 1, the wave amplitudes satisfy the reflection principle

$$A_+(\tau,\eta|r) = \sum_{n=0}^{\infty} r^n A_+(\tau,\eta+n|0), \qquad N_+(\tau,\eta|r) = \sum_{n=0}^{\infty} r^n N_+(\tau,\eta+n|0). \tag{9}$$

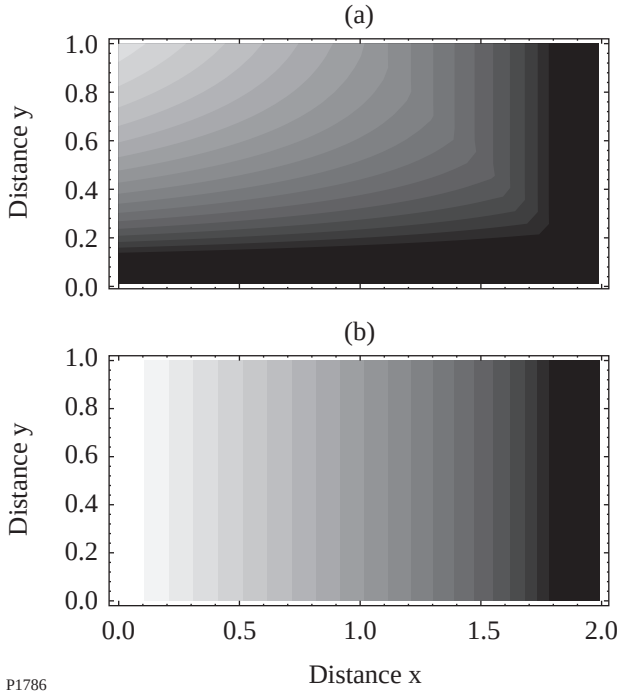

Figure 71.25
Contour plots of the logarithm of the Stokes intensity for cases in which ct/l = 2 and $\gamma_0 l/c$ = 2. White corresponds to high intensity and black corresponds to low intensity. (a) r = 0; (b) r = 1.

For $0 \le \eta \le 1$ the fundamental solutions $A_+(\tau,\eta|0)$ and $N_+(\tau,\eta|0)$ are given by Eqs. (6). For $\eta > 1$ the fundamental solutions are zero until $\tau = \eta - 1$. Subsequently,

$$A_+(\tau,\eta|0) = \begin{cases} \sinh(\gamma\tau) - \sum_{n=0}^{\infty} F_{2n+1}(\tau,\eta-1), \\ \sum_{n=0}^{\infty} F_{2n+1}(\tau,\eta) - \sum_{n=0}^{\infty} F_{2n+1}(\tau,\eta-1), \end{cases}$$

$$N_+(\tau,\eta|0) = \begin{cases} \cosh(\gamma\tau) - \sum_{n=0}^{\infty} F_{2n}(\tau,\eta-1), \\ \sum_{n=0}^{\infty} F_{2n}(\tau,\eta) - \sum_{n=0}^{\infty} F_{2n}(\tau,\eta-1), \end{cases} \quad (10)$$

where the first forms are valid for $\eta - 1 < \tau \le \eta$ and the second forms are valid for $\tau > \eta$. The modification of solutions (6) described by Eqs. (10) is associated with a pulse of infinite width and the initial condition $N_+(0,\eta) = H(1-\eta)$, where H is the Heaviside step function. At early times, the wave amplitudes grow exponentially in time with growth rate γ_0. At intermediate and late times the solutions involve doubly infinite sums of Bessel functions that represent the fundamental contributions to the wave amplitudes and the contributions caused by reflections at the pulse boundaries. A snapshot of the Stokes amplitude described by the exact Eqs. (6), (9), and (10) is displayed in Fig. 71.26(a) for the case in which $r = 0.5$, $ct/l = 2$, and $\gamma_0 l/c = 2$. By comparing Figs. 71.25(a) and 71.26(a), one can see that reflections do not affect the wave evolution in the region $y \ge ct - x$. Reflections affect the wave evolution significantly in the region $y < ct - x$. Despite the complexity of solutions (9), by analyzing the Laplace-transformed solutions from which they originated one can show that, at late times,

$$A_+(\tau,\eta|r) \approx \frac{\gamma(1-r)\exp(\nu\eta + \lambda\tau)}{\nu(2\lambda+\nu)},$$

$$N_+(\tau,\eta|r) \approx \frac{\gamma^2(1-r)\exp(\nu\eta + \lambda\tau)}{\lambda\nu(2\lambda+\nu)}, \quad (11)$$

where

$$\lambda = -\nu/2 + \left(\gamma^2 + \nu^2/4\right)^{1/2} \quad (12)$$

is the growth rate and

$$\nu = -\log r \quad (13)$$

characterizes the convective loss of Stokes light through the pulse boundaries. A snapshot of the Stokes amplitude described by the approximate Eqs. (11)–(13) is displayed in Fig. 71.26(b). Although the approximate solutions (11) are inaccurate near the leading edge of the pulse, as one should expect, they are extremely accurate in the body of the pulse. The growth rate (12) is plotted as a function of r in Fig. 71.27 for the case in which $\gamma_0 l/c = 2$. For this case $r = 0.05$ is

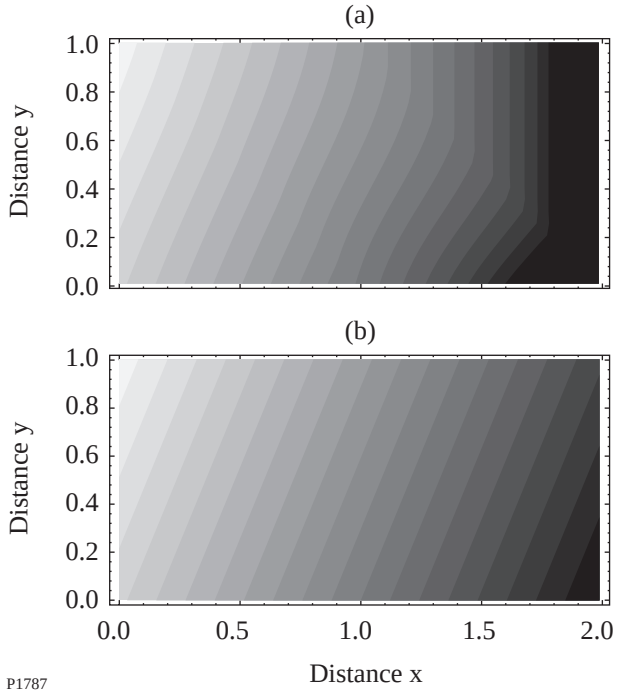

Figure 71.26
Contour plots of the logarithm of the Stokes intensity for the case in which $ct/l = 2$, $\gamma_0 l/c = 2$, and $r = 0.5$. White corresponds to high intensity and black corresponds to low intensity. (a) Exact solution described by Eqs. (6), (9), and (10); (b) approximate solution described by Eqs. (11)–(13).

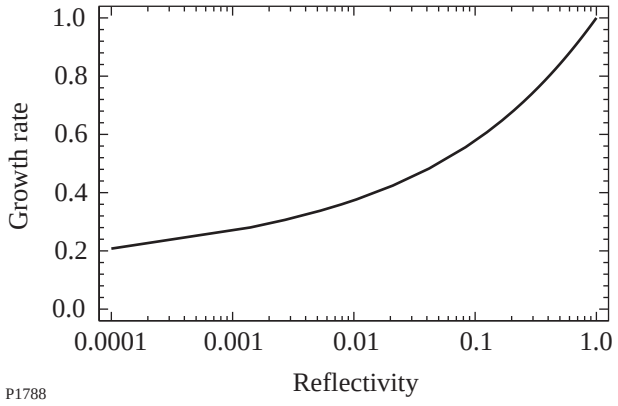

Figure 71.27
Normalized growth rate [Eq. (12)] plotted as a function of r for the case in which $\gamma_0 l/c = 2$.

sufficient to maintain exponential growth with $\lambda = 0.5\gamma$. In general, $r = \exp(-3\gamma/2)$ is sufficient to maintain this rate of exponential growth. Thus, *even weak reflections enhance the growth of sideward SRS significantly*.

Physical Model

Because of the significance of Eqs. (11)–(13), it is important to understand the physical principles on which they are based. The eigenmodes of a fiber are formed by internal reflection, and their existence is not predicated on the existence of SRS.[16] These facts prompt the solution of Eqs. (3) and (5), with $\gamma = 0$. Subject to the initial conditions

$$A_{\pm}(0,\eta) = 1, \tag{14}$$

the solution of these equations is

$$A_{+}(\tau,\eta) = \sum_{n=0}^{\infty} r^{n}\left[H(\tau+1-\eta-n) - H(\tau-\eta-n)\right]. \tag{15}$$

Solution (15) is displayed in Fig. 71.28, together with the function

$$A_{+}(\tau,\eta) = \left[(1-r)/\nu\right]\exp(\nu\eta - \nu\tau), \tag{16}$$

which is the fundamental term in the residue series expansion of solution (15). Because of the tendency of the Stokes wave to propagate out of the plasma, the Stokes amplitude at the right boundary is reduced by a factor of $1/r = \exp(\nu)$ when $\tau = n$. The continuous function $\exp(-\nu\tau)$ captures this essential feature of the temporal wave evolution. When $\tau \neq n$, the right part of the Stokes wave has experienced one less reflection than the left part. Consequently, the Stokes amplitude at the right boundary is larger than the Stokes amplitude at the left boundary by a factor of $1/r$. The continuous function $\exp(\nu\eta)$ captures this essential feature of the spatial wave evolution. If one substitutes the ansatz $A_{+}(\tau,\eta) = a_{+}(\tau)\exp(\nu\eta)$ in Eqs. (3) and (5), with $\gamma = 0$, one finds that the wave amplitude decays exponentially in time, with decay rate ν, in agreement with Eq. (16). Similarly, if one substitutes the ansaetze $A_{+}(\tau,\eta) = a_{+}(\tau)\exp(\nu\eta)$ and $N_{+} = n_{+}(\tau)\exp(\nu\eta)$ in Eqs. (3) and (5), with $\gamma \neq 0$, one finds that the wave amplitudes grow exponentially in time, with growth rate $\lambda = -\nu/2 + \left(\gamma^2 + \nu^2/4\right)^{1/2}$, in agreement with Eq. (12). Thus, solutions (11) are consistent with the formation of a spatial eigenmode that grows in the presence of the pulse.

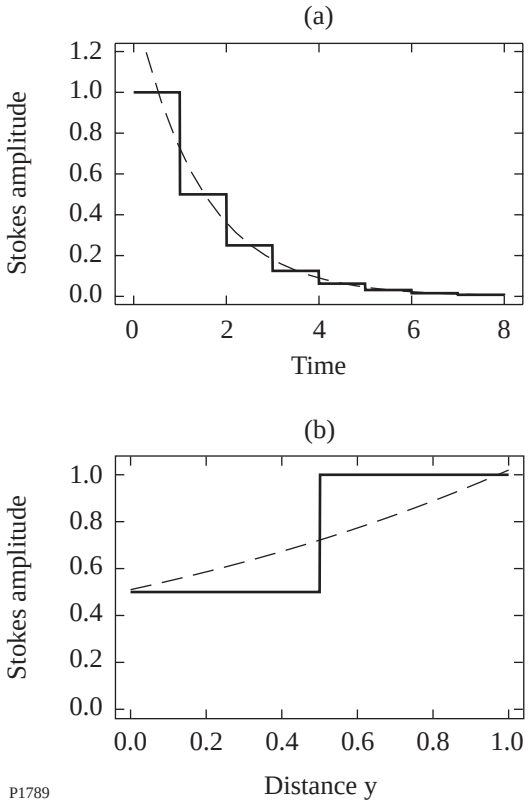

Figure 71.28
Evolution of the Stokes wave for the case in which $\gamma_0 l/c = 2$. The solid lines denote the exact solution (15) and the broken lines denote the approximate solution (16). (a) Stokes amplitude at $y/l = 1$ plotted as a function of ct/l; (b) Stokes amplitude at $ct/l = 0.5$ plotted as a function of y/l.

Summary

In summary, we studied the spatiotemporal evolution of sideward SRS in the weak-coupling regime. In a uniform plasma the sideward convection of the Stokes wave inhibits the growth of sideward SRS. In a plasma channel the partial reflection of Stokes light by the channel walls allows a spatial eigenmode to form in the body of the laser pulse. After this eigenmode has formed, it grows exponentially in time for the subsequent duration of the pulse. The growth rate (12) depends directly on the reflectivity of the channel walls, which, in turn, depends directly on their height. Even weak reflections enhance the growth of sideward SRS significantly. We also made a preliminary analysis of sideward SRS in the strong-coupling regime. Although strong coupling changes the rate at which the instability grows, it does not change the qualitative features of instability growth described herein. In particular, the partial reflection of Stokes light by channel walls allows a spatial

eigenmode to form in the body of the pulse, and the ansaetze described after Eq. (16) can be used to determine the rate at which it grows. For channels created by the pulse, the height of the channel walls depends directly on the pulse intensity. However, since pulses of high intensity evacuate the channel completely, sideward SRS is most important for pulses of moderate intensity. In future work we will apply the physical insights gained in this study of sideward SRS to the study of near-forward and near-backward SRS. Reflections are stronger for these instabilities than for sideward SRS because the Stokes waves approach the channel walls at grazing, rather than normal, incidence. A significant amount of near-forward SRS was observed in recent particle-in-cell simulations of pulse propagation in an underdense plasma.[20,21]

ACKNOWLEDGMENT

We acknowledge useful conversations with V. T. Tikhonchuk and E. A. Williams. This work was supported by the National Science Foundation under Contract No. PHY-9415583, the Department of Energy (DOE) Office of Inertial Confinement Fusion under Cooperative Agreement No. DE-FC03-92SF19460, the University of Rochester, and the New York State Energy Research and Development Authority. The support of DOE does not constitute an endorsement by DOE of the views expressed in this article.

REFERENCES

1. W. L. Kruer, *The Physics of Laser Plasma Interactions*, Frontiers in Physics, Vol. 73 (Addison-Wesley, Redwood City, CA, 1988), Chap. 7.
2. J. M. Dawson, Sci. Am. **260**, 54 (1989).
3. R. S. Craxton, R. L. McCrory, and J. M. Soures, Sci. Am. **255**, 68 (1986).
4. M. Tabak *et al*., Phys. Plasmas **1**, 1626 (1994).
5. C. J. McKinstrie and R. Bingham, Phys. Fluids B **4**, 2626 (1992).
6. T. M. Antonsen, Jr. and P. Mora, Phys. Rev. Lett. **69**, 2204 (1992).
7. T. M. Antonsen, Jr. and P. Mora, Phys. Fluids B **5**, 1440 (1993).
8. W. B. Mori *et al*., Phys. Rev. Lett. **72**, 1482 (1994).
9. S. C. Wilks *et al*., Phys. Plasmas **2**, 274 (1995).
10. C. J. McKinstrie, R. Betti, R. E. Giacone, T. Kolber, and E. J. Turano, Phys. Rev. E **51**, 3752 (1995).
11. C. D. Decker *et al*., Phys. Plasmas **3**, 1360 (1996).
12. C. J. McKinstrie and E. J. Turano, Phys. Plasmas **3**, 4683 (1996).
13. C. J. McKinstrie and E. J. Turano, "Spatiotemporal Evolution of Parametric Instabilities Driven by Short Laser Pulses: Two-Dimensional Analysis," to be published in Physics of Plasmas.
14. P. Monot *et al*., Phys. Rev. Lett. **74**, 2953 (1995).
15. H. M. Milchberg *et al*., Phys. Plasmas **3**, 2149 (1996).
16. G. P. Agrawal, *Nonlinear Fiber Optics* (Academic Press, Boston, 1989), Chap. 2.
17. V. L. Ginzburg, *The Propagation of Electromagnetic Waves in Plasmas*, International Series of Monographs on Electromagnetic Waves, Vol. 7 (Pergamon Press, Oxford, 1964), p. 204.
18. When the plasma corrections to the group speeds of the light waves are important, the first of Eqs. (2) becomes $(\partial_t \pm v_1\partial_y)\, A_\pm = \gamma_0 N_\pm$, where v_1 is the group speed of the Stokes waves and $\gamma_0 = \omega_2 c|\mathbf{k}_2|A_0/4\left[\left(\omega_0 - \omega_2\right)\omega_2\right]^{1/2}$, and the characteristic variables become $\tau = (v_0 t - x)/l$ and $v_0 y/v_1 l$. Equations (3)–(5) are unchanged.
19. For sideward SRS in an underdense plasma, $\gamma_0 l/c \approx 2.2(n_e/n_c)^{1/4}(l/\lambda_0)(v_0/c)$, where λ_0 is the laser wavelength and v_0 is the quiver speed of electrons oscillating in the laser field. One possible set of parameters for which $\gamma_0 l/c \approx 2$ is $n_e/n_c = 0.01$, $l/\lambda_0 = 10$, and $v_0/c = 0.3$.
20. C. D. Decker, W. B. Mori, and T. Katsouleas, Phys. Rev. E **50**, R3338 (1994).
21. K.-C. Tzeng, W. B. Mori, and C. D. Decker, Phys. Rev. Lett. **76**, 3332 (1996).